

# Quasi-Clique Discovery via Energy Diffusion

Yu Zhang<sup>1</sup>, Yilong Luo<sup>1</sup>, Mingyuan Ma<sup>1</sup>, Yao Chen<sup>2</sup>, Enqiang Zhu<sup>3</sup>, Jin Xu<sup>1</sup> and Chanjuan Liu<sup>4</sup>

<sup>1</sup>School of Computing Science, Peking University, Beijing, 100871, China.

<sup>2</sup>Beijing Capital International Airport Co., Ltd., Beijing, China

<sup>3</sup>Institution of Computing Science and Technology, Guangzhou University, China

<sup>4</sup>School of Computer Science and Technology, Dalian University of Technology, China  
yuzhang.cs@stu.pku.edu.cn, zhuenqiang@gzhu.edu.cn, chanjuanliu@dlut.edu.cn

## Abstract

Discovering quasi-cliques—subgraphs whose edge density exceeds a given threshold—is a fundamental task in graph mining with applications to web spam detection, fraud screening, and e-commerce recommendation. However, existing methods for quasi-clique discovery on large-scale web graphs are often sensitive to random seeds or lack of explicit edge-density guarantees, making the task challenging in practice. This paper presents EDQC, an energy diffusion-based method for quasi-clique discovery. EDQC first employs an adaptive energy diffusion process to generate an energy ranking that highlights structurally cohesive regions. Guided by this energy ranking, the algorithm identifies a high-quality subgraph by minimizing conductance, a standard measure from community detection. This subgraph is then refined to meet the specified density threshold. Extensive experiments on 75 real-world graphs show that EDQC finds larger quasi-cliques on most datasets, with consistently lower variance across runs and competitive runtime. To the best of our knowledge, EDQC is the first method to incorporate energy diffusion into quasi-clique discovery.

## 1 Introduction

Dense subgraph models are fundamental to graph mining on large-scale web graphs, enabling web spam detection [1, 2], fraud screening [3, 4], and e-commerce recommendation [5, 6]. Among these models, the *clique* represents the most stringent form, requiring that every pair of vertices be directly connected to each other [7]. However, due to noise and missing links in real-world graphs, exact cliques are rarely observed. To relax this strict requirement, several approximate dense subgraph models have been proposed, including *quasi-cliques* [8, 9], *k-clubs* [10], and *k-plexes* [11]. In particular, the  $\gamma$ -*quasi-clique*, defined by a minimum edge-density threshold, is one of the most widely adopted formulations [12, 13, 14].

Given an undirected graph  $G$  and an edge-density threshold  $\gamma \in (0, 1]$ , the Maximum Quasi-Clique Problem (MQCP) seeks the largest vertex set  $S$  such that the induced subgraph

$G[S]$  exhibits an edge density of at least  $\gamma$ . This edge-density criterion provides a more direct measure of structural cohesion compared to the degree-based definitions utilized by methods such as FastQC [15] and IterQC [16]. However, the MQCP is NP-hard even for fixed values of  $\gamma$  [17] and does not possess the *hereditary property* that allows for efficient pruning in problems related to cliques [18]. Nonetheless, quasi-clique discovery remains highly valuable, as real-world graphs typically exhibit dense yet incomplete connectivity rather than perfect cliques, making quasi-cliques crucial for identifying significant or anomalous substructures.

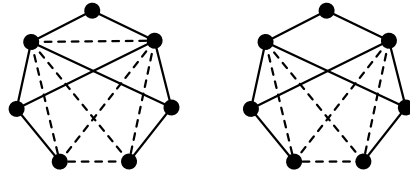


Figure 1: A clique and a 0.8-quasi-clique.

One practical application of quasi-clique discovery is identifying link farm spam pages in web graphs [13], where densely connected spam pages form  $\gamma$ -quasi-cliques, enabling the identification of suspicious link farms even under noise and missing links. As shown in Figure 1, the *dashed* edges in the left subgraph form a size-4 clique, representing a fully connected link farm. In the right subgraph, the dashed edges form a 0.8-quasi-clique, still suspicious despite one missing link, capturing a potential link farm under partial observation or evasion.

Despite recent progress, discovering quasi-cliques in real large-scale web graphs remains challenging due to both scale and combinatorial complexity. While exact algorithms for MQCP, typically based on integer programming or techniques such as branch-and-bound [19, 20, 21, 22], guarantee optimal solutions, their exponential time complexity restricts their applicability to large graphs. As a practical alternative, numerous heuristic methods have been proposed to enable scalable quasi-clique discovery, which can be roughly grouped into four categories. First, *greedy expansion techniques*, such as the greedy strategy with local refinement introduced in [23] and the restart-enabled search in RIG\* [24], prioritize speed but are vulnerable to becoming

ing trapped in local optima. Second, *metaheuristic frameworks* like TSQC [25] and OBMA [26] employ tabu search and opposition-based learning, offering enhanced robustness at a higher computational cost. Third, *local search algorithms*, including NuQClq [12] and its variants NuQClqF1 and NuQClqR1 [14], utilize bounded configuration checking and adaptive rules for candidate refinement. However, despite their sophisticated local optimizations, these methods often exhibit instability due to their dependence on random seeds. Lastly, *similarity-based heuristics* such as NBSim and its accelerated variant, FastNBSim, utilize vertex neighborhood overlap to identify and expand quasi-cliques [13]. While both methods are highly efficient, FastNBSim introduces MinHash-based approximations, making it sensitive to random seeds and potentially less stable. Moreover, neither method supports a user-specified edge-density threshold. Instead, the edge-density of the returned subgraph emerges implicitly from similarity parameters. Consequently, there is no guarantee that the output meets a specified minimum edge-density requirement. This limits their suitability for applications that require strict control over quasi-clique edge-density thresholds.

Among these four categories, local search and similarity-based methods have been the most competitive for discovering large quasi-cliques. The state-of-the-art algorithms for MQCP include NBSim and its accelerated variant, FastNBSim [13], as well as the local search algorithms NuQClqF1 and NuQClqR1 [14]. However, these methods remain sensitive to random seeds or lack of explicit edge-density guarantees.

*Energy diffusion* is a natural candidate for addressing the challenges above. Diffusion methods such as PageRank [27] and the heat kernel [28] have shown strong performance on structure-aware tasks, e.g., vertex ranking and community detection [29, 30], where diffused mass tends to localize within cohesive regions. These tasks overlap with quasi-clique discovery in highlighting tightly interlinked vertices, yet they are not equivalent because quasi-cliques must satisfy a specified minimum edge-density on induced subgraphs. This connection motivates exploring energy diffusion for quasi-clique discovery to reduce sensitivity to random seeds in practice and to furnish a stable candidate region for density-constrained extraction.

This paper introduces EDQC, an energy diffusion-based method for quasi-clique discovery. EDQC begins with an adaptive energy diffusion phase, where the energy transfer rate is dynamically adjusted based on the local energy distribution. This phase runs for a fixed number of iterations from each source vertex, generating an *energy ranking* that highlights structurally cohesive regions. Guided by this energy ranking, EDQC then employs a principled extraction mechanism from community detection theory. It applies a *sweep cut* to the energy-ranked vertices to identify a high-quality subgraph that minimizes *conductance*. This subgraph is subsequently refined through a structure-driven procedure to guarantee it meets the specified density threshold. Extensive experiments on 75 real-world graphs, including classic web graphs, demonstrate that EDQC discovers larger quasi-cliques on most datasets, with consistently lower variance and

competitive runtime. To the best of our knowledge, EDQC is the first method to incorporate energy diffusion into quasi-clique discovery.

## 2 Preliminaries

All graphs considered in this paper are undirected and simple (no loops or parallel edges). Let  $G = (V, E)$  represent a graph with a *vertex set*  $V$  and an *edge set*  $E$ . Two vertices  $u$  and  $v$  within  $V$  are termed *adjacent* if  $uv \in E$ , and one vertex is referred to as a *neighbor* of the other. The set of all neighbors for a vertex  $u$  is known as its *neighborhood*, denoted  $N(u)$ , while the *closed neighborhood* of  $u$  is denoted  $N[u] = N(u) \cup \{u\}$ . The *degree* of a vertex  $u$ , denoted as  $d(u)$ , indicates the number of its neighbors, i.e.,  $d(u) = |N(u)|$ .

Let  $n = |V|$  and  $m = |E|$ . For a vertex set  $S \subseteq V$ , the *induced subgraph* is  $G[S]$  with vertex set  $S$  and edge set  $E(S) = \{\{u, v\} \in E \mid u, v \in S\}$ . Let  $m(S) = |E(S)|$  denote the number of *internal edges* in  $G[S]$ , and define the *internal degree* of  $u \in S$  by

$$d_S(u) = |N(u) \cap S|.$$

The *edge density* of  $S$  (and of  $G[S]$ ) is

$$\eta(S) = \begin{cases} \frac{2m(S)}{|S|(|S| - 1)}, & |S| \geq 2, \\ 0, & \text{otherwise,} \end{cases}$$

and  $\eta(G)$  is shorthand for  $\eta(V)$ . Throughout this paper, unless otherwise stated, *density* means edge density.

**Definition 1** ( $\gamma$ -Quasi-Clique). *Given  $G = (V, E)$  and a density threshold  $\gamma \in (0, 1]$ . A vertex set  $S \subseteq V$  induces a  $\gamma$ -quasi-clique if the induced subgraph  $G[S]$  has edge density at least  $\gamma$ , i.e.,*

$$\eta(G[S]) \geq \gamma.$$

*For brevity, we also refer to  $G[S]$  itself as a  $\gamma$ -quasi-clique. A  $\gamma$ -quasi-clique  $G[S]$  is maximal if there is no  $v \in V \setminus S$  such that  $\eta(G[S \cup \{v\}]) \geq \gamma$ .*

**Definition 2** (Maximum Quasi-Clique Problem). *Given  $G = (V, E)$  and a density threshold  $\gamma \in (0, 1]$ , the Maximum Quasi-Clique Problem (MQCP) seeks*

$$S^* \in \arg \max_{S \subseteq V} \left\{ |S| \mid \eta(G[S]) \geq \gamma \right\}.$$

*The induced subgraph  $G[S^*]$  is a maximum  $\gamma$ -quasi-clique. When  $\gamma = 1$ , MQCP reduces to the classical Maximum Clique Problem. For any fixed  $\gamma$ , MQCP is NP-hard and may admit multiple optimal solutions [17].*

**Definition 3** (Conductance). *Conductance is a standard measure used to evaluate how well a vertex set forms a community [31]. For a non-empty, proper subset of vertices  $S \subset V$ , its volume is defined as  $\text{vol}(S) = \sum_{u \in S} d(u)$ , and the cut between  $S$  and its complement is  $\text{cut}(S, V \setminus S) = |\{\{u, v\} \in E \mid u \in S, v \in V \setminus S\}|$ . The conductance of  $S$  is then:*

$$\Phi(S) = \frac{\text{cut}(S, V \setminus S)}{\min(\text{vol}(S), \text{vol}(V \setminus S))}.$$

*A lower conductance value indicates a more clearly defined community, signifying few edges connecting the set to the rest of the graph relative to its internal connectivity.*

---

**Algorithm 1:** EDQC( $G, \gamma, T, \theta$ )

---

**Input:** Graph  $G = (V, E)$ , density threshold  $\gamma$ , diffusion rounds  $T$ , activation threshold  $\theta$

**Output:** Vertex set  $S^*$  of a large  $\gamma$ -quasi-clique

```
1  $S^* \leftarrow \emptyset$ ;  
2 foreach  $v \in V$  in non-increasing order of degree do  
3    $f \leftarrow \text{ENERGYDIFFUSION}(G, v, T, \theta)$ ;  
4    $S \leftarrow \text{EXTRACTQUASICLIQUE}(G, f, \gamma, \theta)$ ;  
5   if  $|S| > |S^*|$  then  
6      $S^* \leftarrow S$ ;  
7 return  $S^*$ 
```

---

### 3 The EDQC Algorithm

This section details the proposed Energy Diffusion-based Quasi-Clique discovery (EDQC) algorithm. Given a graph  $G = (V, E)$  and a density threshold  $\gamma$ , EDQC identifies a large vertex set  $S$  that induces a  $\gamma$ -quasi-clique. The overall pipeline is outlined in Algorithm 1.

The algorithm iterates through vertices, treating each as a source to initiate a two-stage process. First, an adaptive energy diffusion process generates an energy distribution over the graph. Second, guided by this energy distribution, a principled extraction mechanism identifies a high-quality quasi-clique. EDQC maintains the largest quasi-clique found across all source vertices. Processing vertices in non-increasing degree order is an efficiency heuristic [32], as it ensures high-degree vertices are processed as energy sources first, thereby increasing the likelihood of finding a large quasi-clique early in the search.

#### 3.1 Adaptive Energy Diffusion

The first stage, detailed in Algorithm 2, simulates the diffusion of energy from a source vertex  $v$  over  $T$  synchronous rounds. The goal is to produce an energy function  $f : V \rightarrow \mathbb{R}_{\geq 0}$  where energy is concentrated in structurally cohesive regions surrounding the source.

The diffusion process is designed to be adaptive. The fraction of energy a vertex releases depends on its current energy relative to its neighborhood, a dynamic governed by an adaptive fraction  $\alpha(u)$ . This design is deliberate and distinct from standard diffusion mechanisms such as the heat kernel [28] or PageRank [27], which often treat connections uniformly. Our adaptive fraction makes the diffusion process sensitive to the evolving energy landscape, enabling EDQC to be more conservative in sparse regions and more aggressive within dense ones.

The diffusion starts by initializing a unit energy at the source vertex  $v$  (line 1). In each of the  $T$  synchronous rounds (lines 2–14), the algorithm first identifies the set of *active vertices*,  $A$ , based on the activation threshold  $\theta$  (line 3). To ensure updates are synchronous, a temporary copy of the energy function,  $f'$ , is created (line 4). The diffusion rule is then applied to each active vertex  $u \in A$  with a non-zero degree ( $d(u) > 0$ ). Isolated vertices are skipped as they have no neighbors to which energy can be transferred, a condition necessary for the conservation of total energy. For each such

---

**Algorithm 2:** ENERGYDIFFUSION( $G, v, T, \theta$ )

---

**Input:** Graph  $G = (V, E)$ , source vertex  $v$ , diffusion rounds  $T$ , activation threshold  $\theta$

**Output:** Energy function  $f : V \rightarrow \mathbb{R}_{\geq 0}$

```
1 Initialize  $f(v) \leftarrow 1$  and  $f(x) \leftarrow 0$  for  $x \neq v$ ;  
2 for  $t = 1$  to  $T$  do  
3    $A \leftarrow \{x \in V \mid f(x) > \theta\}$ ;  
4    $f' \leftarrow f$ ;  
5   foreach  $u \in A$  do  
6     if  $d(u) > 0$  then  
7        $\alpha(u) \leftarrow \frac{\sum_{w \in N(u)} f(w) + f(u)}{\sum_{w \in N(u)} f(w) + 2f(u)}$ ;  
8        $\delta(u) \leftarrow \alpha(u)f(u)$ ;  
9       Sample  $\xi_{uw} \sim \text{Exp}(1)$  for each  
10         $w \in N(u)$ ;  
11         $\phi_{uw} \leftarrow \frac{\xi_{uw}}{\sum_{x \in N(u)} \xi_{ux}}$  for each  $w \in N(u)$ ;  
12         $f'(u) \leftarrow f'(u) - \delta(u)$ ;  
13        foreach  $w \in N(u)$  do  
14           $f'(w) \leftarrow f'(w) + \delta(u)\phi_{uw}$ ;  
15 return  $f$ 
```

---

vertex  $u \in A$  (line 5), the algorithm computes its adaptive fraction  $\alpha(u)$  and the total energy to transfer,  $\delta(u)$  (lines 7–8). This energy is then stochastically allocated among its neighbors using weights  $\phi_{uw}$  derived from an exponential distribution (lines 9–10). Subsequently, the energies of the active vertex and its neighbors are updated in the temporary function  $f'$  (lines 11–13). After all active vertices have been processed, the energy function  $f$  is updated with the temporary copy, completing the round (line 14).

**Properties.** This diffusion process has several key properties.

**Proposition 1** (Energy Conservation). *The total energy is conserved in each round:  $\sum_{x \in V} f'(x) = \sum_{x \in V} f(x)$ .*

*Proof.* Consider a fixed round and an arbitrary active vertex  $u$  where  $d(u) > 0$ . The synchronous updates associated with  $u$  results in a change of  $-\delta(u)$  for  $u$  and an addition of  $\delta(u)\phi_{uw}$  for each neighbor  $w \in N(u)$ , satisfying  $\sum_{w \in N(u)} \phi_{uw} = 1$ . Therefore,  $\delta(u) = \sum_{w \in N(u)} \delta(u)\phi_{uw}$ . Summing over all active vertices leads to the conclusion that  $\sum_{x \in V} f'(x) = \sum_{x \in V} f(x)$ . Here, we should note that the energy of vertices for which  $d(u) = 0$  or  $f(u) = 0$  remains unchanged in the energy diffusion process.  $\square$

The conservation of energy is a crucial property for the algorithm's stability. It guarantees that the process only redistributes the initial energy, rather than arbitrarily creating or losing it, thus ensuring a fair basis for comparing the energy distributions originating from different source vertices.

**Proposition 2** (Properties of  $\alpha(u)$ ). *For an active vertex  $u$  with  $f(u) > 0$  and  $d(u) > 0$ , the adaptive fraction  $\alpha(u) \in [1/2, 1)$  and is monotonically increasing with the total energy of its neighbors,  $S(u) = \sum_{w \in N(u)} f(w)$ .*

*Proof.* We begin by rewriting the formula for  $\alpha(u)$  (line 7, Algorithm 2) as  $\alpha(u) = 1 - \frac{f(u)}{S(u)+2f(u)}$ . Since  $S(u) \geq 0$  and  $f(u) > 0$  for an active vertex, the denominator  $S(u) + 2f(u)$  is strictly positive. The fractional term is bounded by  $0 < \frac{f(u)}{S(u)+2f(u)} \leq \frac{f(u)}{2f(u)} = 1/2$ . Consequently,  $\alpha(u)$  is bounded by  $1 - 1/2 \leq \alpha(u) < 1 - 0$ , which gives  $\alpha(u) \in [1/2, 1)$ . For monotonicity, the partial derivative with respect to  $S(u)$  is:

$$\frac{\partial \alpha(u)}{\partial S(u)} = \frac{f(u)}{(S(u) + 2f(u))^2} > 0.$$

This confirms that  $\alpha(u)$  is strictly increasing with  $S(u)$ .  $\square$

The adaptive nature of our diffusion is formally established by this proposition. The bounds on  $\alpha(u)$  guarantee a process that is both consistently active and stable, preventing the diffusion from stalling. Concurrently, the monotonicity is the key mechanism driving the algorithm’s core premise: it mathematically ensures that energy is exchanged more readily within already high-energy (and thus likely dense) regions, accelerating the concentration of energy.

**Proposition 3** (Unbiased Distribution in Expectation). *The expected fraction of energy that an active vertex  $u$  transfers to a specific neighbor  $w \in N(u)$  is uniform across all neighbors:  $\mathbb{E}[\phi_{uw}] = 1/d(u)$ .*

*Proof.* The weights  $\phi_{uw}$  are derived by normalizing i.i.d. exponential random variables  $(\xi_{uw})_{w \in N(u)}$ . This construction is a standard method for generating a random point from a uniform distribution on the standard simplex. By symmetry, the expectation of each component is identical. Since  $\sum_{w \in N(u)} \phi_{uw} = 1$ , by linearity of expectation,  $\sum_{w \in N(u)} \mathbb{E}[\phi_{uw}] = 1$ . As there are  $d(u)$  identical terms in the sum, it follows that  $d(u) \cdot \mathbb{E}[\phi_{uw}] = 1$ , which proves  $\mathbb{E}[\phi_{uw}] = 1/d(u)$ .  $\square$

While the exponential sampling introduces stochasticity to explore different structural paths, this proposition guarantees that the process remains unbiased in expectation. On average, all neighbors are treated fairly, ensuring that the algorithm itself introduces no arbitrary structural bias during the diffusion.

**Theorem 1** (Complexity of Algorithm 2). *The ENERGYDIFFUSION algorithm runs in  $O(T(n + m))$  time.*

*Proof.* The algorithm performs  $T$  rounds. We analyze the computational cost of a single round. First, identifying the active set  $A$  requires a full scan of all vertices, which takes  $O(n)$  time. Next, the algorithm iterates through each active vertex  $u \in A$ . For each such vertex, all calculations—including the summations for  $\alpha(u)$  and  $\phi_{uw}$ , and the subsequent updates—are proportional to its degree,  $d(u)$ . Therefore, the total work for processing all active vertices in a round is bounded by the sum of degrees of all vertices in the graph, which is  $\sum_{u \in V} O(d(u)) = O(m)$ . Summing the costs within a single round gives a complexity of  $O(n + m)$ . As the process repeats for  $T$  rounds, the total complexity of the algorithm is  $O(T(n + m))$ .  $\square$

## 3.2 Quasi-Clique Extraction

The second stage of EDQC takes the final energy function  $f$  returned by Algorithm 2 and produces a vertex set  $S$  that induces a  $\gamma$ -quasi-clique. This extraction process (Algorithm 3) has three main operations: an initial ranking of vertices, the identification of a high-quality initial subgraph, and a refinement procedure.

First, the algorithm identifies the set of active vertices  $A$  and sorts them in descending order of their energy scores to create an ordered sequence  $P$  (lines 1–2). This ranking is crucial, as it places vertices most likely to belong to a cohesive community at the forefront.

Next, to identify a high-quality initial candidate set, the algorithm performs a sweep cut [31] on the energy-ranked list  $P$  (line 3). This procedure examines the nested prefixes of the list and selects the one that minimizes conductance, as it represents the most well-defined community structure. This strategy is highly effective because the initial energy ranking provides a high-quality vertex permutation. It is a known principle in local graph clustering that sweep cuts perform best when applied to an ordering that places vertices from the same community contiguously [31]. Our energy diffusion process is designed for precisely this purpose: it creates an ordering where structurally cohesive vertices are naturally placed at the top. This, in turn, enables the sweep cut to accurately identify the boundary of the best candidate subgraph.

Finally, this initial set  $S$  undergoes a refinement procedure (lines 4–15). The refinement begins with a pruning loop (lines 4–6). If the initial set  $S$  does not meet the density threshold, this loop iteratively removes the vertex with the minimum internal degree  $d_S(u)$  until the set  $S$  induces a valid  $\gamma$ -quasi-clique. Following this, an expansion phase seeks to enlarge the set (lines 8–15). In each pass, the remaining candidates  $R$  are re-sorted based on their connectivity to the current set  $S$  (line 10). The algorithm then iterates through this sorted list  $R$ , attempting to greedily add the first vertex  $v$  that maintains the density constraint (lines 12–13). Upon a successful insertion, the current iteration over the candidate list is immediately terminated (line 15), allowing the algorithm to restart the process with an up-to-date candidate ranking in the next iteration.

**Theorem 2** (Complexity of Algorithm 3). *Let  $k = |A|$  be the number of active vertices. The EXTRACTQUASICLIQUE stage runs in  $O(k^2 + m(A))$ , where  $m(A)$  is the number of edges in the induced subgraph  $G[A]$ .*

*Proof.* The overall complexity is determined by the main steps of the algorithm. Sorting the  $k$  active vertices takes  $O(k \log k)$  time. The subsequent sweep cut, which involves calculating conductance for  $k$  prefixes, can be implemented in  $O(m(A))$  time with incremental updates for the cut and volume. The final refinement stage is the most computationally intensive. The pruning and expansion loops can, in the worst case, lead to a series of  $O(k)$  vertex additions or removals. With incremental maintenance of internal degrees and edge counts, each step of these loops can take up to  $O(k)$  time to find the best candidate to remove or to scan through remaining candidates for addition. This results in a worst-case complexity of  $O(k^2)$  for the refinement phase. Summing these

---

**Algorithm 3:** EXTRACTQUASICLIQUE( $G, f, \gamma, \theta$ )

---

**Input:** Graph  $G = (V, E)$ , energy function  $f$ , density threshold  $\gamma$ , activation threshold  $\theta$

**Output:** A vertex set  $S$  that induces a  $\gamma$ -quasi-clique

```
1  $A \leftarrow \{v \in V \mid f(v) > \theta\}$ ;  
2  $P \leftarrow$  vertices of  $A$  sorted by decreasing  $f$ ;  
3  $S \leftarrow \arg \min_{i \in \{1, \dots, |P|\}} \Phi(\{v_1, \dots, v_i\}$  where  $v_i \in P$ );  
4 while  $|S| > 1$  and  $\eta(G[S]) < \gamma$  do  
5    $u \leftarrow \arg \min_{x \in S} d_S(x)$ ;  
6    $S \leftarrow S \setminus \{u\}$ ;  
7  $changed \leftarrow \mathbf{true}$ ;  
8 while  $changed$  do  
9    $changed \leftarrow \mathbf{false}$ ;  
10   $R \leftarrow$  vertices of  $P \setminus S$ , sorted by connections to  $S$ ;  
11  foreach  $v \in R$  do  
12    if  $\eta(G[S \cup \{v\}]) \geq \gamma$  then  
13       $S \leftarrow S \cup \{v\}$ ;  
14       $changed \leftarrow \mathbf{true}$ ;  
15      break;  
16 return  $S$ 
```

---

costs, the total complexity is  $O(k \log k + m(A) + k^2)$ , which simplifies to  $O(k^2 + m(A))$ .  $\square$

**Theorem 3** (Complexity of EDQC). *The theoretical worst-case time complexity of the EDQC algorithm (Algorithm 1) is  $O(n^3)$ .*

*Proof.* The algorithm’s main loop iterates up to  $n$  times. Each iteration calls two procedures: ENERGYDIFFUSION, with a complexity of  $O(T(n + m))$ , and EXTRACTQUASICLIQUE, with a worst-case complexity of  $O(n^2 + m)$ . As  $T$  is a small constant, the cost of a single iteration is dominated by the extraction step, at  $O(n^2 + m)$ . Therefore, the total worst-case complexity is  $O(n^3 + nm)$ . Since  $m = O(n^2)$  for any simple graph, this simplifies to  $O(n^3)$ . The initial sorting of vertices by non-increasing degree is a lower-order term that does not affect this bound.

We note that this is a theoretical worst-case analysis. In practice, EDQC is run as a time-bounded heuristic, and its empirical efficiency is demonstrated in our experimental section.  $\square$

## 4 Experimental Evaluation

We conducted a comprehensive experimental evaluation to validate the performance and robustness of EDQC. This section is organized as follows. We first detail the experimental setup, the baseline methods, and the datasets used. We then present the main results on effectiveness and efficiency, followed by a statistical analysis to confirm the significance of our findings. Subsequently, we provide an in-depth analysis of the algorithm, including an ablation study to verify the contribution of its key components and an empirical study to validate its core premise. The section concludes with a summary of our parameter sensitivity analysis.

### 4.1 Experimental Setup

All methods were implemented in C++ and compiled with g++ 9.4.0 using the ‘-O3’ optimization flag. The experiments were conducted on a machine equipped with an AMD EPYC 7H12 CPU (1.5 GHz base frequency) and 128 GB of RAM, running Ubuntu 20.04.

Each baseline was run with the parameter settings recommended in its original paper. For EDQC, we fixed the diffusion rounds at  $T = 2$  and the activation threshold at  $\theta = 10^{-4}$ . These values were selected based on a sensitivity study, the details of which are provided in Section 4.8.

Due to inherent randomness, all non-deterministic methods (all except NBSim) were executed 10 times with random seeds from 1 to 10; NBSim, being deterministic, was run once. For the non-deterministic methods, we report their average quasi-clique size and standard deviation (STD) over the 10 runs, presented in the format ‘average size  $\pm$  STD’, where the standard deviation is reported only if it is non-zero. All runs were subject to a 60-second timeout. If an algorithm failed to find any valid  $\gamma$ -quasi-clique in all 10 runs for an instance, we mark its result as ‘N/A’. The 60-second timeout reflects common practice in recent time-bounded heuristic studies [33, 34].

### 4.2 Baseline Methods

We compared EDQC against four state-of-the-art algorithms:

- **NBSim/FastNBSim** [13]: Similarity-based heuristics that expand subgraphs based on neighborhood overlap. FastNBSim accelerates NBSim via MinHash-based approximation.
- **NuQClqF1/NuQClqR1** [14]: Advanced variants of NuQClq [12]. These algorithms employ information feedback models that integrate historical solutions using fitness-weighted scores to guide local search.

### 4.3 Datasets

We evaluated all algorithms on 75 real-world datasets from SNAP [35] and the Network Repository [36]. The collection covers diverse domains, including web, social, and communication graphs. The datasets span a wide spectrum of scales, with vertex counts ( $n$ ) ranging from 62 to over 16.7 million, and edge densities spanning from  $8.41 \times 10^{-2}$  down to as low as  $1.87 \times 10^{-7}$ . This diversity provided a challenging testbed for evaluating the scalability and effectiveness of the algorithms.

### 4.4 Main Results

We now present the primary results comparing the effectiveness and efficiency of EDQC against the baselines. A key challenge in this comparison is that NBSim and FastNBSim do not accept a density threshold  $\gamma$  as input. To facilitate a fair evaluation, we designed two separate experimental settings (Table 1 and Table 2). To save space, we omit instances where all four compared algorithms found solutions of the same average size.

Table 1: Quasi-clique sizes with the threshold  $\gamma$  set by NBSim’s output.

Instance	$\gamma$	NBSim	NuQClqF1	NuQClqR1	EDQC
rt-retweet	1	3	4	4	4
web-polblogs	1	5	9	9	9
email-Eu-core	1	12	18	18	18
ego-facebook	0.99	71	92	92	92
ca-Erdos992	1	6	8	8	8
socfb-CMU	0.98	20	53	53	53
ech-WHOIS	0.98	57	79	79	79
web-indochina-2004	1	50	49 ± 3.16	50	50
socfb-UCSB37	0.99	40	64	64	64
socfb-UConn	0.99	22	58	58	58
socfb-UCLA	0.79	19	96	96	96
socfb-Berkeley13	1	21	42	42	42
socfb-Wisconsin87	0.98	12	46	46	46
soc-epinions	1	10	16	16	16
Cit-HepTh	1	12	22.9 ± 0.32	23	23
socfb-Indiana	0.85	27	94	94	94
socfb-Ullinois	1	14	57	57	57
Cit-HepPh	0.98	14	23	23	23
socfb-UF	0.99	24	67	66.8 ± 0.63	67
Email-Enron	0.97	10	25	25	25
socfb-Penn94	0.98	14	56	55.3 ± 2.21	56
soc-brightkite	0.99	36	45	45	45
socfb-OR	0.6	19	108	108	108
soc-slashdot	1	12	26	26	26
witter_combined	0.98	79	89.3 ± 11.7	89.3 ± 11.7	93
G_n.pin.pout	1	3	4	4	4
yahoo-msg	0.99	22	20.6 ± 2.07	20.6 ± 2.01	23
soc-douban	1	5	11	11	11
wave	1	5	6	6	6
Loc-Gowalla	0.99	31	23.8 ± 2.53	23	31
soc-gowalla	0.99	31	23	23.8 ± 2.53	31
web-Stanford	0.99	67	64.2 ± 3.43	59.9 ± 4.12	67.5 ± 0.71
cnr-2000	0.99	89	84.8 ± 3.61	81.8 ± 0.63	89
web-NotreDame	1	155	154.3 ± 0.48	154.2 ± 0.42	155
ca-MathSciNet	1	25	24.6 ± 0.84	24.7 ± 0.67	25
coPapersDBLP	1	337	333.5 ± 4.12	333.5 ± 4.12	337
auto	1	6	7	7	7
web-it-2004	1	432	431.8 ± 0.42	432	432
soc-delicious	0.58	22	80	80	80
ca-coauthors-dblp	1	337	333.5 ± 4.12	333.5 ± 4.12	337
eu-2005	0.99	405	191.3 ± 115.84	127.2 ± 26.92	405.1 ± 0.32
web-Google	0.99	48	39.2 ± 7.86	39.5 ± 7.41	48
rgg_n.2.20.s0	0.57	17	41	41	40.2 ± 0.79
rgg_n.2.21.s0	1	18	18.1 ± 0.57	18.1 ± 0.57	19
rgg_n.2.22.s0	1	19	18.8 ± 0.79	18.6 ± 0.7	20
rgg_n.2.23.s0	0.99	19	18.3 ± 0.48	19 ± 1.41	22
rgg_n.2.24.s0	0.98	20	19.7 ± 0.95	18.7 ± 0.48	23

**Effectiveness and Stability.** The results in Table 1 and Table 2 show the superior effectiveness and stability of EDQC. A quantitative summary highlights this advantage. In the first setting (Table 1), across the 47 instances where results differed, EDQC achieves or ties for the best average size in 46 instances. This compares favorably to the other methods, where NuQClqR1 achieved or tied for the best size in 29 instances, followed by NuQClqF1 (28 instances) and NBSim (10 instances). Similarly, in the second setting (Table 2), EDQC achieves or ties for the best size in 68 out of 69 instances. For comparison, the counts for the other algorithms were: NuQClqR1 (46 instances), NuQClqF1 (45 instances), and FastNBSim (2 instances).

Beyond average size, EDQC demonstrates exceptional stability. It consistently reports a standard deviation close to zero (e.g., 0.32 on the large eu-2005 graph), even on complex instances. This is in stark contrast to the NuQClq variants, which frequently exhibit high variance on the same instances (e.g., a STD of 115.84 for NuQClqF1 on eu-2005). Furthermore, the results highlight the unreliability of the similarity-based methods. FastNBSim, for instance, often fails to achieve its own best-found density (succeeding only

Table 2: Quasi-clique sizes with  $\gamma$  set by FastNBSim’s max density over 10 runs. For FastNBSim, stats are on successful runs only (rate shown in parentheses).

Instance	$\gamma$	FastNBSim	NuQClqF1	NuQClqR1	EDQC
soc-dolphins	0.83	4 (4/10)	6	6	6
rt-retweet	1	3 (7/10)	4	4	4
ca-netscience	1	8.1 ± 0.88 (10/10)	9	9	9
web-polblogs	0.93	6 (2/10)	13	13	13
rt-twitter-copen	1	3.6 ± 0.53 (7/10)	4	4	4
email-Eu-core	0.94	21 (1/10)	29	29	29
web-edu	1	27.4 ± 3.1 (10/10)	30	30	30
ego-facebook	0.96	102 (1/10)	123	123	123
ca-GrQc	1	37.8 ± 3.2 (4/10)	44	44	44
web-spam	1	15.5 ± 0.71 (2/10)	20	20	20
ca-Erdos992	1	5 (6/10)	8	8	8
socfb-CMU	0.97	28 (1/10)	56	56	56
ech-WHOIS	0.96	73 (1/10)	91	91	91
ca-HepPh	1	202.7 ± 24.04 (10/10)	239	239	239
web-indochina-2004	1	49.9 ± 0.32 (10/10)	49 ± 3.16	50	50
web-BerkStan	1	26.7 ± 2.83 (10/10)	29	29	29
socfb-UCSB37	0.98	47 (1/10)	70	70	70
web-webbase-2001	1	32.9 ± 0.32 (10/10)	33	33	33
socfb-UConn	0.97	34 (1/10)	65	65	65
ca-AstroPh	1	51.8 ± 3.12 (10/10)	57	57	57
socfb-UCLA	0.98	49 (1/10)	63	63	63
ca-CondMat	1	22.63 ± 2.83 (8/10)	26	26	26
socfb-Berkeley13	0.95	29 (1/10)	62	62	62
socfb-Wisconsin87	0.91	34 (1/10)	65	65	65
soc-epinions	0.95	16 (1/10)	21	21	21
Cit-HepTh	0.92	26 (1/10)	41	41	41
socfb-Indiana	0.95	40 (1/10)	71	70.8 ± 0.63	71
socfb-Ullinois	0.94	48 (1/10)	92	92	92
Cit-HepPh	0.98	20 (1/10)	23	23	23
socfb-UF	0.94	69 (1/10)	93	93	93
Email-Enron	0.96	13 (1/10)	26	26	26
socfb-Penn94	0.94	42 (1/10)	63.4 ± 3.37	63.3 ± 3.59	65
soc-brightkite	0.97	43 (1/10)	53	53	53
socfb-OR	0.92	24 (1/10)	50.9 ± 0.32	50.9 ± 0.32	51
soc-slashdot	0.97	10 (1/10)	35	35	35
wordnet-words	1	29.2 ± 2.71 (6/10)	32	32	32
witter_combined	0.97	87 (1/10)	99	99	99
G_n.pin.pout	0.5	4 (3/10)	7.9 ± 0.32	7.9 ± 0.32	8
yahoo-msg	0.96	24 (1/10)	23.4 ± 1.84	23.9 ± 1.1	25
web-sk-2005	0.99	83 (3/10)	84	84	84
soc-douban	0.72	9 (1/10)	23	23	23
wave	0.71	8 (3/10)	14	14	14
web-arabic-2005	1	90.7 ± 5.36 (10/10)	102	102	102
Loc-Gowalla	1	23.5 ± 0.71 (2/10)	21	21	29
soc-gowalla	0.99	25 (1/10)	23	23.8 ± 2.53	31
ca-dblp-2010	1	70.6 ± 4.86 (10/10)	75	75	75
ca-citeseer	1	81.6 ± 5.36 (10/10)	87	87	87
coAuthorsCiteseer	1	81.6 ± 5.36 (10/10)	87	87	87
web-Stanford	0.99	62 (1/10)	64.2 ± 3.43	59.9 ± 4.12	67.5 ± 0.71
coAuthorsDBLP	1	103 ± 9.7 (10/10)	115	115	115
ca-dblp-2012	1	104 ± 9.52 (10/10)	114	114	114
com-dblp	1	101.4 ± 5.76 (10/10)	114	114	114
cnr-2000	1	84 (1/10)	81.9 ± 1.45	81.8 ± 1.55	84
web-NotreDame	1	153.5 ± 1.43 (10/10)	154.3 ± 0.48	154.2 ± 0.42	155
ca-MathSciNet	1	23.8 ± 0.79 (10/10)	24.6 ± 0.84	24.5 ± 0.85	25
coPapersDBLP	1	316.9 ± 23 (10/10)	333 ± 3.94	333 ± 3.94	337
auto	0.77	9.5 ± 0.71 (2/10)	11	11	11
web-it-2004	1	431.7 ± 0.48 (10/10)	431.8 ± 0.42	432	432
soc-delicious	0.88	30 (1/10)	31.4 ± 3.86	31.4 ± 3.86	37
ca-coauthors-dblp	1	316.9 ± 23 (10/10)	333.5 ± 4.12	330.2 ± 10.01	337
soc-digg	0.9	76 (1/10)	104 ± 13.7	98.8 ± 12.56	116.9 ± 0.32
eu-2005	0.99	387 (1/10)	191.3 ± 115.84	127.2 ± 26.92	405.1 ± 0.32
web-Google	1	40.7 ± 3.21 (3/10)	33.7 ± 2.63	37.1 ± 6.08	44
soc-pokec	0.99	31 (1/10)	24.6 ± 2.37	23.8 ± 1.55	25
rgg_n.2.22.s0	0.98	19 (1/10)	20.1 ± 0.99	20 ± 0.94	21
rgg_n.2.23.s0	0.99	21 (1/10)	18.3 ± 0.48	19 ± 1.41	22
hugetrace-00010	0.5	4 (10/10)	N/A	N/A	5
hugetrace-00020	0.5	4 (10/10)	N/A	N/A	5
rgg_n.2.24.s0	0.95	20 (1/10)	20.6 ± 1.26	20.9 ± 1.37	25

1/10 times on many graphs). This lack of explicit density control makes them less suitable for applications requiring highly cohesive structures, a task where EDQC’s reliability is a distinct advantage.

**Efficiency.** The efficiency of EDQC is compared against baselines in Figure 2, where, following prior work [37], instances where the runtime of both algorithms is below 0.1 seconds are excluded. On this log-log plot, points falling below the 1×, 10×, and 100× lines indicate that EDQC is faster than the baseline by the corresponding factor or more. The results clearly show that EDQC is substantially more efficient than the high-performing local search methods, NuQClqF1 and NuQClqR1, with a large number of points falling below

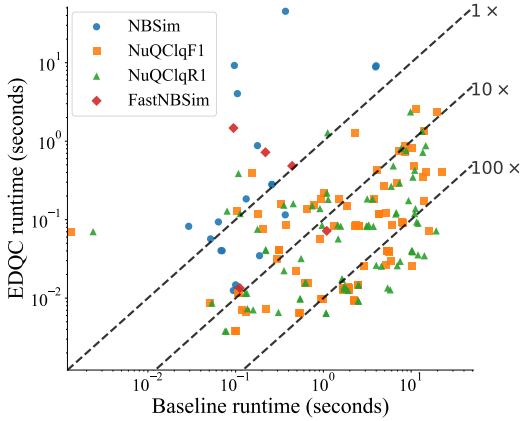


Figure 2: Runtime comparison of EDQC against baselines on a log-log scale.

the  $10\times$  line, signifying a speedup of over an order of magnitude. In comparison to the fast similarity-based heuristics (NBSim and FastNBSim), EDQC’s runtime remains highly competitive, as most of their corresponding points cluster around the  $1\times$  line. Overall, this demonstrates that EDQC strikes an excellent balance between achieving state-of-the-art solution quality and maintaining high computational efficiency.

#### 4.5 Statistical Analysis

To assess statistical significance, we applied the Friedman test [38] on the algorithm rankings across all 75 datasets. The null hypothesis that all algorithms perform equally was rejected in both settings ( $p < 0.05$ ), allowing us to proceed with the post-hoc Nemenyi test [39] to identify pairwise performance differences.

The results are visualized using Critical Difference (CD) diagrams in Figure 3. In these diagrams, algorithms are plotted on an axis according to their average rank across all datasets; a lower rank (further to the left) is better. Groups of algorithms whose performance is not statistically significantly different are connected by a horizontal bar, the length

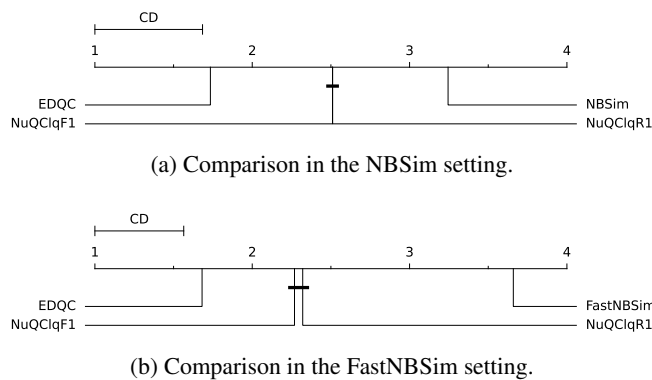


Figure 3: Critical Difference diagrams for algorithm ranks on all 75 datasets (significance level 0.05). A horizontal bar connects algorithms with no statistically significant difference.

of which corresponds to the critical difference.

The top plot in Figure 3 shows the comparison for the NBSim setting. EDQC achieves the best average rank, and this leading position is statistically significant. The post-hoc test reveals that EDQC’s performance is significantly better than all three other baselines: NuQClqF1, NuQClqR1, and NBSim. A similar trend is observed in the FastNBSim setting, shown in the bottom plot. Once again, EDQC obtains the best average rank. Its superiority is also confirmed to be statistically significant, as it significantly outperforms NuQClqF1, NuQClqR1, and FastNBSim.

In summary, the statistical tests provide conclusive evidence for the superiority of EDQC. In both experimental settings, EDQC not only achieves the best average rank but also demonstrates a statistically significant performance advantage over all compared state-of-the-art baselines. These results provide strong statistical evidence that EDQC represents a reliably superior approach for this task.

#### 4.6 Analysis of EDQC Components

To isolate and verify the contribution of each key component, we conducted an ablation study comparing the full EDQC against five variants across 112 unique experimental settings (consolidating settings where both configurations yielded the same  $\gamma$  value). These variants were designed to test the core aspects of our algorithm: the subgraph identification strategy (EDQC-1), the energy-guided ranking (EDQC-2, EDQC-3), the refinement phase (EDQC-4), and the nature of the diffusion process itself (EDQC-5).

The results, summarized in Table 3, provide conclusive evidence that each component is essential for EDQC’s superior performance. The most dramatic performance degradation occurred with EDQC-5, which replaced our adaptive diffusion with a naive random process, and EDQC-1, which substituted conductance-based identification with a max-density heuristic. The full EDQC algorithm proved superior in 106 and 69 instances, respectively. These results underscore that our principled diffusion and extraction mechanisms form the foundational pillars of the algorithm’s success. The importance of the energy-guided ranking was also clearly demonstrated; disrupting the descending energy order with a random (EDQC-2) or ascending (EDQC-3) ranking severely hampered performance, leading to 56 and 70 wins for the full EDQC. Finally, disabling the refinement phase (EDQC-4) also resulted in a noticeable performance drop in 16 instances, confirming that this final step is vital for optimizing the solution size.

Additionally, we confirmed the robustness of our synchronous design. As variants with a fixed processing order for active vertices produced identical results to the full EDQC, the order-independence guaranteed by the synchronous design was empirically verified.

#### 4.7 Empirical Validation of the Energy-Density Premise

To empirically validate our algorithm’s core premise that energy concentrates in dense regions, we analyzed the relationship between subgraph density and energy retention on eight representative datasets. For each dataset, we compared the

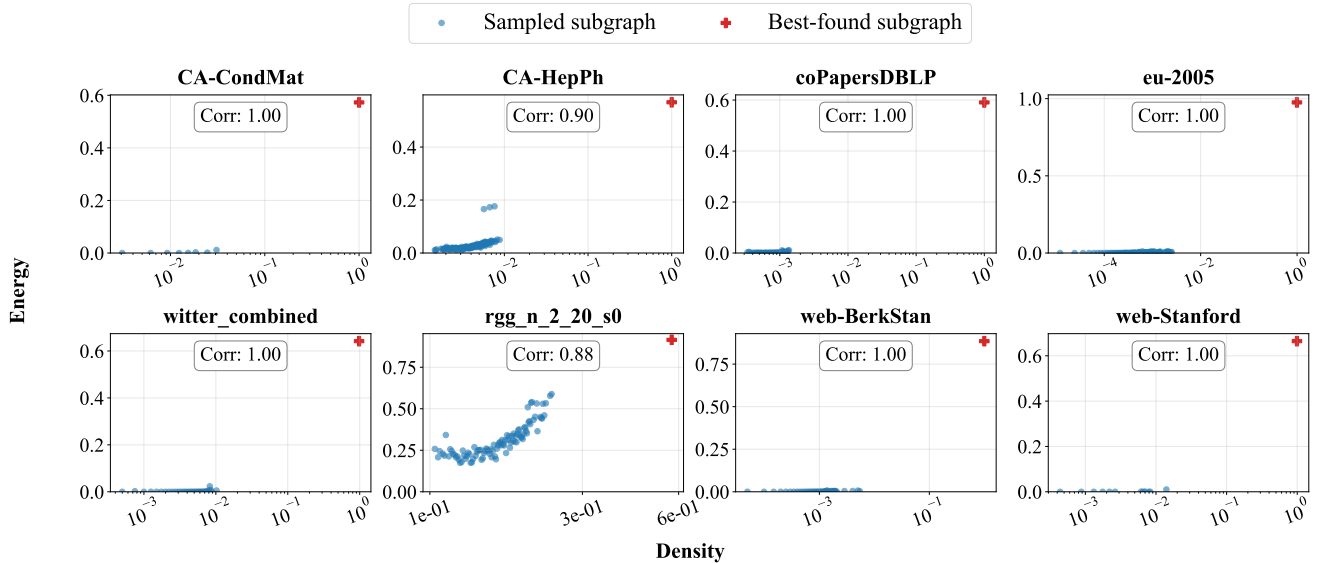


Figure 4: Subgraph density vs. total retained energy on eight representative datasets. Each blue dot represents one of 1,000 randomly sampled subgraphs of a fixed size; the red marks the quasi-clique of the same size found by EDQC.

Table 3: Comparison of the full EDQC with its five simplified variants across 112 experimental settings. #bet and #wor represent the number of instances where EDQC achieves better and worse quasi-clique sizes, respectively.

Variant	Description	#bet (EDQC $\hat{c}$ Variant)	#wor (EDQC $\hat{c}$ Variant)
EDQC-1	No Conductance	69	0
EDQC-2	Random Ranking	56	1
EDQC-3	Ascending Ranking	70	1
EDQC-4	No Refinement Phase	16	1
EDQC-5	Naive Random Diffusion	106	0

quasi-clique found by EDQC against 1,000 randomly sampled subgraphs of the same size. The results, visualized in Figure 4, reveal a strong positive correlation between density and retained energy, confirmed by high Pearson correlation coefficients (typically  $> 0.90$ ). More importantly, the quasi-clique discovered by EDQC (red marks) consistently appears as a top-right outlier, indicating that it captures a disproportionately high amount of energy even among other subgraphs of similar density. This strong alignment provides the empirical justification for using the energy ranking as a powerful guide in the discovery of quasi-cliques.

#### 4.8 Parameter Sensitivity

This section provides the detailed results of our parameter sensitivity analysis, which was designed to evaluate the impact of the number of diffusion rounds  $T$  and the activation threshold  $\theta$  on EDQC’s performance. For this study, we selected three representative datasets to cover different scales: *ego-facebook* (a small graph,  $|V| \leq 10^4$ ), *rgg\_n\_2\_19\_s0* (a medium graph,  $10^4 < |V| \leq 10^6$ ), and *web-Google* (a large graph,  $|V| > 10^6$ ).

On each of these graphs, we evaluated EDQC by testing 15 combinations of  $T \in \{1, 2, 3\}$  and  $\theta \in \{10^{-4}, 5 \times$

$10^{-3}, 5 \times 10^{-3}, 10^{-2}\}$ . This evaluation was repeated under three different density thresholds,  $\gamma \in \{0.7, 0.8, 0.9\}$ , to ensure a comprehensive analysis. We report both the discovered quasi-clique size and the runtime for each configuration. The results for the small, medium, and large graphs are presented in Figure 5–7.

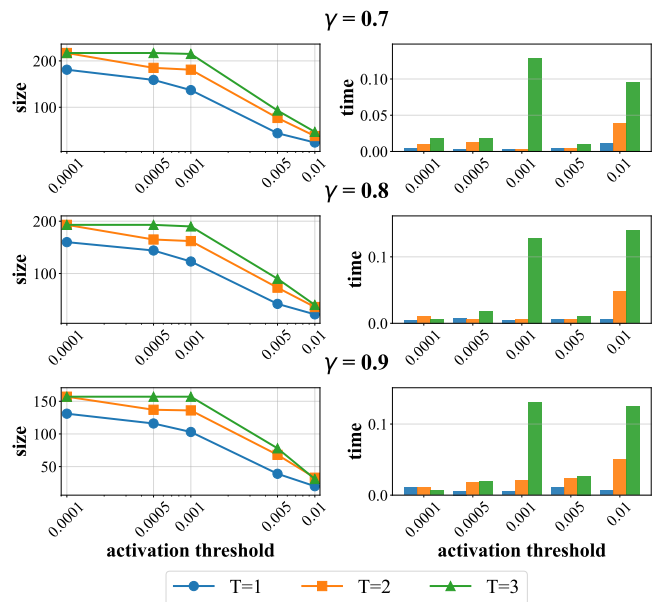


Figure 5: Parameter sensitivity analysis for EDQC on the small representative graph (*ego-facebook*). Each of the three rows corresponds to a different density threshold  $\gamma$ . For each  $\gamma$ , the left plot shows the resulting quasi-clique size versus the activation threshold  $\theta$  (on a log scale), and the right plot shows the corresponding runtime.

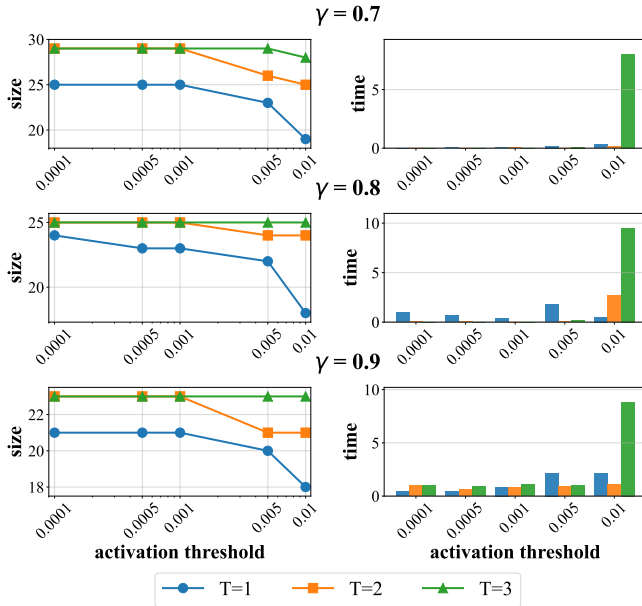


Figure 6: Parameter sensitivity analysis on the medium representative graph (`rgg_n2_19_s0`). The layout of the plots is identical to that described in the caption of Figure 5.

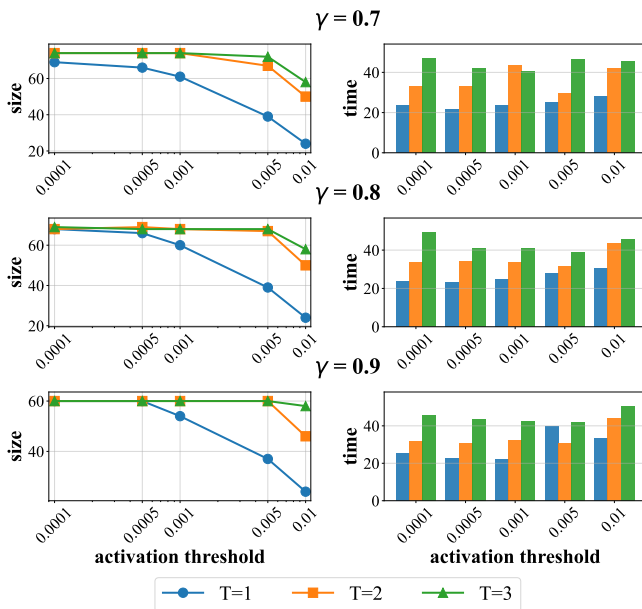


Figure 7: Parameter sensitivity analysis on the large representative graph (`web-Google`). The layout of the plots is identical to that described in the caption of Figure 5.

Across all three datasets, a consistent pattern emerges. In terms of solution quality (size), configurations with  $T = 2$  and  $T = 3$  consistently and significantly outperform  $T = 1$ , especially for smaller values of the activation threshold ( $\theta \leq 10^{-3}$ ). As  $\theta$  increases, making vertex activation stricter, the performance of all settings tends to decline. Regarding efficiency, the runtime plots clearly show that the computational cost increases with  $T$ . While  $T = 3$  occasionally finds a marginally larger quasi-clique than  $T = 2$ , its runtime is substantially higher across all settings. For instance, in the large graph setting (Figure 7), the runtime for  $T = 3$  can be several times that of  $T = 2$  for little to no improvement in solution size.

Based on this analysis, we conclude that the configuration  $T = 2$  provides the best trade-off between solution quality and computational cost. Paired with a small activation threshold such as  $\theta = 10^{-4}$ , which consistently lies in the stable, high-performance region shown in the plots, this configuration represents an effective and efficient choice. This justifies our use of  $T = 2$  and  $\theta = 10^{-4}$  for all main experiments presented in the paper.

## 5 Conclusion

In this paper, we introduced EDQC, a novel algorithm for quasi-clique discovery designed to mitigate key limitations of existing methods, such as their sensitivity to random seeds and lack of explicit edge-density guarantees. We demonstrated that the effectiveness of EDQC stems from its two-stage design. First, an adaptive energy diffusion process generates an energy ranking that highlights structurally cohesive regions. Then, guided by this ranking, a principled extraction mechanism based on conductance minimization identifies and refines a high-quality subgraph. To the best of our knowledge, EDQC is the first method to incorporate energy diffusion into this task, offering a robust alternative to traditional heuristics.

Our extensive experiments on 75 real-world graphs confirmed the effectiveness of this approach. The results demonstrated that EDQC finds larger quasi-cliques on most datasets, with consistently lower variance across runs, highlighting its superior stability. Furthermore, statistical tests confirmed the significance of these findings, and our analysis showed that EDQC maintains a competitive runtime, striking an excellent balance between solution quality and efficiency.

Future work can extend the EDQC framework in several promising directions. Generalizing the diffusion model for weighted and attributed graphs is an important next step. Applying EDQC to downstream tasks, such as anomaly detection in financial networks and community detection in social graphs, could further validate its practical utility. Finally, exploring more advanced refinement strategies may lead to further improvements in solution quality.

## References

- [1] David Gibson, Ravi Kumar, and Andrew Tomkins. Discovering large dense subgraphs in massive graphs. In *Proceedings of the 31st international conference on Very large data bases*, pages 721–732, 2005.

- [2] Longlong Lin, Pingpeng Yuan, Rong-Hua Li, Jifei Wang, Ling Liu, and Hai Jin. Mining stable quasi-cliques on temporal networks. *IEEE Transactions on Systems, Man, and Cybernetics: Systems*, 52(6):3731–3745, 2021.
- [3] Yuyan Zheng, Chuan Shi, Xiangnan Kong, and Yanfang Ye. Author set identification via quasi-clique discovery. In *Proceedings of the 28th ACM International Conference on Information and Knowledge Management*, pages 771–780, 2019.
- [4] Yixiang Fang, Wensheng Luo, and Chenhao Ma. Densest subgraph discovery on large graphs: Applications, challenges, and techniques. *Proceedings of the VLDB Endowment*, 15(12):3766–3769, 2022.
- [5] J Ben Schafer, Joseph A Konstan, and John Riedl. E-commerce recommendation applications. *Data mining and knowledge discovery*, 5(1):115–153, 2001.
- [6] Junshuai Song, Xiaoru Qu, Zehong Hu, Zhao Li, Jun Gao, and Ji Zhang. A subgraph-based knowledge reasoning method for collective fraud detection in e-commerce. *Neurocomputing*, 461:587–597, 2021.
- [7] Hiroo Saito, Masashi Toyoda, Masaru Kitsuregawa, and Kazuyuki Aihara. A large-scale study of link spam detection by graph algorithms. In *Proceedings of the 3rd international workshop on Adversarial information retrieval on the web*, pages 45–48, 2007.
- [8] James Abello, Mauricio GC Resende, and Sandra Sudarsky. Massive quasi-clique detection. In *Latin American symposium on theoretical informatics*, pages 598–612. Springer, 2002.
- [9] Jian Pei, Daxin Jiang, and Aidong Zhang. On mining cross-graph quasi-cliques. In *Proceedings of the eleventh ACM SIGKDD international conference on Knowledge discovery in data mining*, pages 228–238, 2005.
- [10] Robert J Mokken et al. Cliques, clubs and clans. *Quality & Quantity*, 13(2):161–173, 1979.
- [11] Stephen B Seidman and Brian L Foster. A graph-theoretic generalization of the clique concept. *Journal of Mathematical sociology*, 6(1):139–154, 1978.
- [12] Jiejiang Chen, Shaowei Cai, Shiwei Pan, Yiyuan Wang, Qingwei Lin, Mengyu Zhao, and Minghao Yin. Nuqclq: An effective local search algorithm for maximum quasi-clique problem. In *Proceedings of the AAAI Conference on Artificial Intelligence*, volume 35, pages 12258–12266, 2021.
- [13] Jiayang Pang, Chenhao Ma, and Yixiang Fang. A similarity-based approach for efficient large quasi-clique detection. In *Proceedings of the ACM Web Conference 2024*, pages 401–409, 2024.
- [14] Shuhong Liu, Jincheng Zhou, Dan Wang, Zaijun Zhang, and Mingjie Lei. An optimization algorithm for maximum quasi-clique problem based on information feedback model. *PeerJ Computer Science*, 10:e2173, 2024.
- [15] Aritra Konar and Nicholas D Sidiropoulos. Optimal quasi-clique: hardness, equivalence with densest-k-subgraph, and quasi-partitioned community mining. In *Proceedings of the AAAI Conference on Artificial Intelligence*, volume 38, pages 8608–8616, 2024.
- [16] Guimei Liu and Limsoon Wong. Effective pruning techniques for mining quasi-cliques. In *Joint European conference on machine learning and knowledge discovery in databases*, pages 33–49. Springer, 2008.
- [17] Jeffrey Pattillo, Alexander Veremyev, Sergiy Butenko, and Vladimir Boginski. On the maximum quasi-clique problem. *Discrete Applied Mathematics*, 161(1-2):244–257, 2013.
- [18] Hongbo Xia, Kaiqiang Yu, Shengxin Liu, Cheng Long, and Xun Zhou. Maximum degree-based quasi-clique search via an iterative framework. *Proceedings of the 31th ACM SIGKDD Conference on Knowledge Discovery and Data Mining*, 2025.
- [19] Takeaki Uno. An efficient algorithm for solving pseudo clique enumeration problem. *Algorithmica*, 56:3–16, 2010.
- [20] Grigory Pastukhov, Alexander Veremyev, Vladimir Boginski, and Oleg A Prokopyev. On maximum degree-based-quasi-clique problem: Complexity and exact approaches. *Networks*, 71(2):136–152, 2018.
- [21] Celso C Ribeiro and José A Riveaux. An exact algorithm for the maximum quasi-clique problem. *International Transactions in Operational Research*, 26(6):2199–2229, 2019.
- [22] Ahsanur Rahman, Kalyan Roy, Ramiza Maliha, and Townim Faisal Chowdhury. A fast exact algorithm to enumerate maximal pseudo-cliques in large sparse graphs. In *Proceedings of the 30th ACM SIGKDD Conference on Knowledge Discovery and Data Mining*, pages 2479–2490, 2024.
- [23] Charalampos Tsourakakis, Francesco Bonchi, Aristides Gionis, Francesco Gullo, and Maria Tsiarli. Denser than the densest subgraph: extracting optimal quasi-cliques with quality guarantees. In *Proceedings of the 19th ACM SIGKDD international conference on Knowledge discovery and data mining*, pages 104–112, 2013.
- [24] AB Oliveira, A Plastino, and CC Ribeiro. Construction heuristics for the maximum cardinality quasi-clique problem. In *10th Metaheuristics International Conference. Singapore*, volume 84, 2013.
- [25] Youcef Djeddi, Hacene Ait Haddadene, and Nabil Belacel. An extension of adaptive multi-start tabu search for the maximum quasi-clique problem. *Computers & Industrial Engineering*, 132:280–292, 2019.
- [26] Qing Zhou, Una Benlic, and Qinghua Wu. An opposition-based memetic algorithm for the maximum quasi-clique problem. *European Journal of Operational Research*, 286(1):63–83, 2020.

- [27] Lawrence Page, Sergey Brin, Rajeev Motwani, and Terry Winograd. The pagerank citation ranking: Bringing order to the web. Technical report, Stanford infolab, 1999.
- [28] Fan Chung. The heat kernel as the pagerank of a graph. *Proceedings of the National Academy of Sciences*, 104(50):19735–19740, 2007.
- [29] Kyle Kloster and David F Gleich. Heat kernel based community detection. In *Proceedings of the 20th ACM SIGKDD international conference on Knowledge discovery and data mining*, pages 1386–1395, 2014.
- [30] David F Gleich, Lek-Heng Lim, and Yongyang Yu. Multilinear pagerank. *SIAM Journal on Matrix Analysis and Applications*, 36(4):1507–1541, 2015.
- [31] Reid Andersen, Fan Chung, and Kevin Lang. Local graph partitioning using pagerank vectors. In *2006 47th annual IEEE symposium on foundations of computer science (FOCS'06)*, pages 475–486. IEEE, 2006.
- [32] Ryan A Rossi, David F Gleich, Assefaw H Gebremedhin, and Md Mostofa Ali Patwary. Fast maximum clique algorithms for large graphs. In *Proceedings of the 23rd International Conference on World Wide Web*, pages 365–366, 2014.
- [33] Jinkun Lin, Shaowei Cai, Chuan Luo, and Kaile Su. A reduction based method for coloring very large graphs. In *Proceedings of the 26th International Joint Conference on Artificial Intelligence*, pages 517–523, 2017.
- [34] Jiongzhi Zheng, Kun He, and Jianrong Zhou. Farsighted probabilistic sampling: A general strategy for boosting local search maxsat solvers. In *Proceedings of the AAAI Conference on Artificial Intelligence*, volume 37, pages 4132–4139, 2023.
- [35] Jure Leskovec and Andrej Krevl. SNAP Datasets: Stanford large network dataset collection, June 2014.
- [36] Ryan A. Rossi and Nesreen K. Ahmed. The network data repository with interactive graph analytics and visualization. In *AAAI*, 2015.
- [37] Rui Sun, Zhaohui Liu, Yiyuan Wang, Han Xiao, Jiangnan Li, and Jiejiang Chen. Numds: An efficient local search algorithm for minimum dominating set problem. In *Proceedings of the 34th International Joint Conference on Artificial Intelligence*, 2025.
- [38] Milton Friedman. The use of ranks to avoid the assumption of normality implicit in the analysis of variance. *Journal of the american statistical association*, 32(200):675–701, 1937.
- [39] Janez Demšar. Statistical comparisons of classifiers over multiple data sets. *Journal of Machine learning research*, 7(Jan):1–30, 2006.